Electronic Supplementary Information

Hydrogen evolution reaction catalyzed by ruthenium ion-complexed graphitic carbon nitride nanosheets

Yi Peng,[a] Bingzhang Lu,[a] Limei Chen,[a] Nan Wang,[b] Jia-En Lu,[a] Yuan Ping,[a,*] and Shaowei Chen[a,*]

[a] Department of Chemistry and Biochemistry, University of California, 1156 High Street, Santa Cruz, CA 95064, USA

[b] New Energy Research Institute, School of Environment and Energy, South China University of Technology, Guangzhou 510006, China

Table S1. Summary of XPS results of C_3N_4, C_3N_4-Ru-F, and C_3N_4-Ru-P

	C 1s (eV)		Ru 3d (eV)		N 1s (eV)		Cl 2p (eV)		Ru:C=N-C	Ru:Cl
	N-C=N	C-C	5/2	3/2	C=N-C	N-C3 or H-N-C2	3/2	1/2		
C_3N_4	287.31	284.06	-	-	397.80	399.58	-		-	-
C_3N_4-Ru-P	287.57	284.27	281.67	285.77	398.08	399.48	197.50	199.00	1:4.7	1:0.48
C_3N_4-Ru-F	287.93	284.2	281.30	285.40	398.48	399.48	197.70	199.20	1:2.0	1:0.51

Table S2. Comparison of the HER performance of C_3N_4-Ru-F and relevant catalysts reported in recent literature.

Catalyst	η_{10} (mV)	Tafel slope (mV/dec)	Loading (mg/cm^2)	J_0 (μA/cm^2)	reference
C_3N_4-Ru-F	-140	57	0.153	72	This work
C_3N_4-Cu	-390	76	0.28	N/A	Appl. Surf. Sci., 2015, 357, 221
C_3N_4-nanoribbon-G	-207	54	0.143	39.8	Angew. Chem. Int. Ed. 2014, 53, 13934
C_3N_4/NG	-240	51.5	0.1	0.35	Nat. Comm. 2014, 5, 3783
Co@NG	-180	79	0.285	NA	Chem. Mater. 2015, 27, 2026
Co-NRCNT	-260	80	0.28	10	Angew. Chem. Int. Ed. 2014, 126, 4461
Co-C-N	-138	55	N/A	N/A	JACS, 2015, 137, 15070
Mo_2C/CNT-GR	-130	58	0.66	63	ACS Nano, 2014, 8, 5164
$Mn_{0.05}Co_{0.95}Se_2$	-195	36	0.28	68.3	JACS, 2016, 138, 5087
$MoS_{0.94}P_{0.53}$	-150	57	0.285	N/A	Adv. Mater., 2016, 28, 1427
WS_2@P,N,O-graphene	-125	52.7	0.159	131	Adv. Mater. 2015, 27, 4234

N,P-C	-163	89	0.3	160	Angew. Chem. Int. Ed. 2016, 128, 2270
MoP	-145	54	N/A	34	Energy Environ. Sci., 2014, 7, 2624
WS$_2$ nanosheets	-230	60	0.1-0.2	20	Nat. Mater., 2013, 12, 850
S,N-C	-116	68	0.285	N/A	Nano Energy, 2015, 16, 357
MoS$_2$/carbon	-159	56	0.285	N/A	Nano Energy, 2016, 22, 490
Au@N-C	-130	77	0.357	N/A	Angew. Chem. Int. Ed., 2016, 128, 8556

Table S3. Summary of XPS results of C$_3$N$_4$-M nanocomposites (M = Fe^{3+}, Co^{3+}, Ni^{3+} and Cu^{2+}).

	2p$_{3/2}$	2p$_{3/2}$ (satellite)	2p$_{1/2}$	2p$_{1/2}$ (satellite)
C$_3$N$_4$-Fe	708.9	713.1	722.1	726.7
C$_3$N$_4$-Co	780.0	795.4	784.7	800.4
C$_3$N$_4$-Ni	855.3	872.3	861.2	878.2
C$_3$N$_4$-Cu	932.7	941.0	952.8	961.6

Table S4. Results of calculated hydrogen adsorption energy (ΔG_{H^*}) of the labeled positions in Figure S14.

Catalyst	Bonding position	Total Energy (eV)	Avib (eV)	ΔE (eV)	ΔG (eV)
C$_3$N$_4$	N	-3142.38029	0.02758272	-0.66004	-0.63245
	C	-3140.52942	0.03672051	1.19083	1.22755
C$_3$N$_4$-Ru	Ru	-5782.20717	0.20015401	-0.69182	-0.49166
	N1	-5781.2634	0.31675791	0.25195	0.56871
	N2	-5781.22813	0.31675791	0.28722	0.60397
	C	-5782.32939	0.33418123	-0.81404	-0.47986

The adsorption free energy (ΔG_{H^*}) is calculated by the following equations,

$$\Delta E = E(^*+H) - (E(^*) + \tfrac{1}{2}E(H_2)); \quad \Delta G = \Delta E + ZPE - T\Delta S$$

where E is the total energy, ΔE is adsorption energy, * is the active site, ΔG is Gibbs free energy, ZPE is the zero point energy, T is temperature and ΔS is the entropy change.
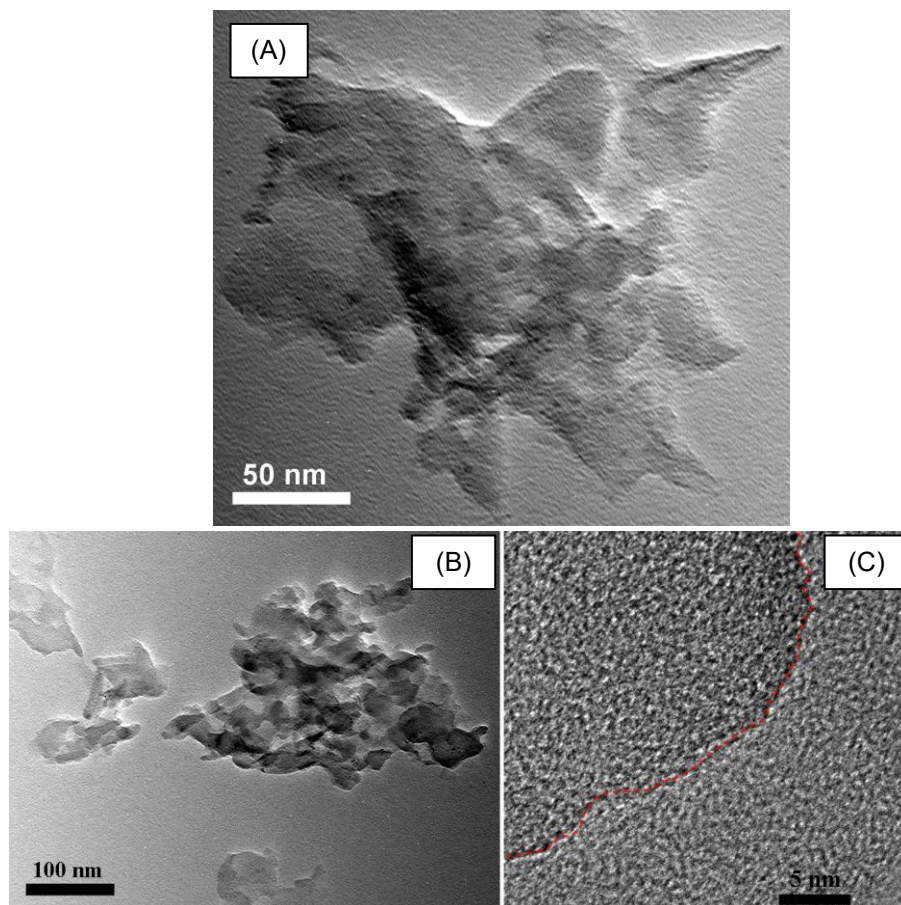
Figure S1. Representative TEM images of (A) graphitic C_3N_4 nanosheets and (B, C) of C_3N_4-Ru-F at varied magnifications. Scale bar is 500 nm in (A), 100 nm in (B) and 5 nm in (C). From Panels (B) and (C), one can see that no Ru or RuO_x nanoparticles are formed.
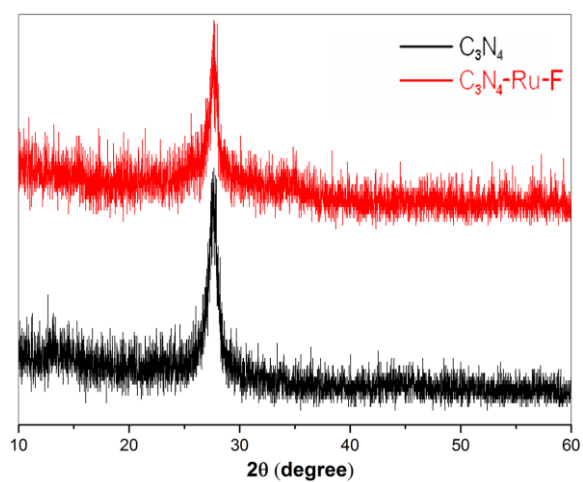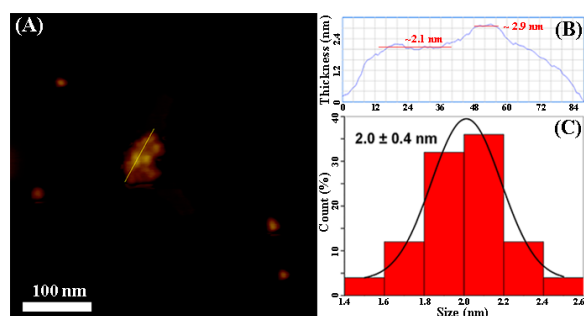

Figure S2. XRD patterns of C_3N_4 and C_3N_4-Ru-F.

Figure S3. (A) Typical AFM topograph of C_3N_4 nanosheets. (B) Height analysis for the line scan in panel (A). (C) Thickness histogram of the C_3N_4 nanosheets based on AFM height measurements as exemplified in panel (A).
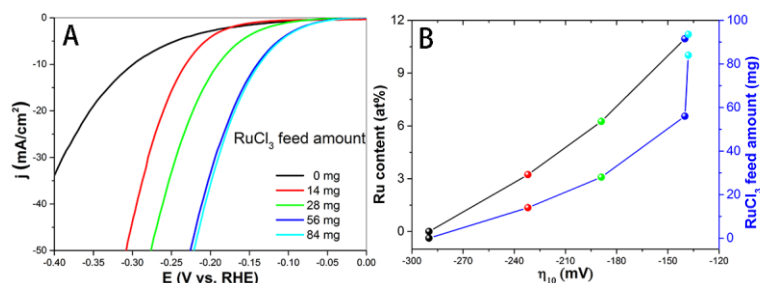
Figure S4. (A) Polarization curves of HER on C_3N_4-Ru in 0.5 M H_2SO_4 where the nanocomposites were prepared with the addition of different amounts of $RuCl_3$ (specified in Figure legends). (B) Variation of η_{10} with the amount of $RuCl_3$ added and Ru content in C_3N_4-Ru nanocomposites quantified by ICP-MS measurements.

To examine the effects of Ru contents on the HER activity, we prepared two additional samples with the addition of 14 and 84 mg of $RuCl_3$, the Ru contents in the corresponding C3N4-Ru composites were determined by both ICP-MS and XPS measurements, as shown in the table below. First, one can see that the Ru content in the C3N4-Ru nanocomposites was almost identical when determined by ICP-MS and XPS measurements. Second, the Ru content increased with the amount of $RuCl_3$ added in the synthesis, and became unchanged when more than 56 mg of $RuCl_3$ was added, suggesting that indeed the sample was saturated with Ru centers. Third, electrochemical measurements did show enhanced HER performance with increasing Ru content in the C3N4-Ru nanocomposites. However, the increase was nonlinear, as depicted in Figure S4.

$RuCl_3$ feed amount (mg)	Ru at.% (ICP-MS)	Ru at.% (XPS)
14	3.23	4.10
28 (C_3N_4-Ru-P)	6.25	7.09
56 (C_3N_4-Ru-F)	10.95	12.50
84	11.20	12.60
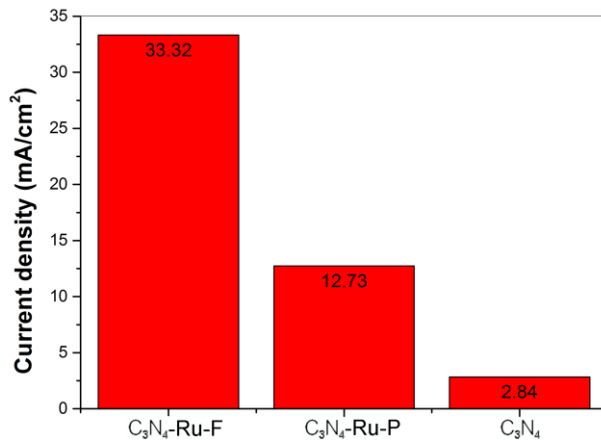
Figure S5. HER current density of C_3N_4-Ru-F, C_3N_4-Ru-P, and C_3N_4 at the overpotential of -200 mV.
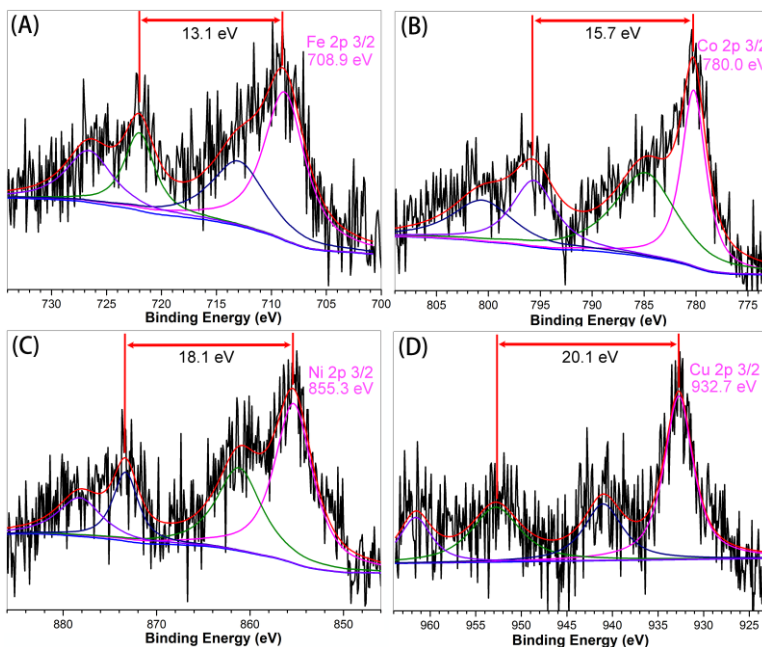
Figure S6. XPS spectra of the C_3N_4-M nanocomposites (M = Fe^{3+}, Co^{3+}, Ni^{3+} and Cu^{2+}): (A) Fe 2p, (B) Co 2p, (C) Ni 2p and (D) Cu 2p. Black curves are experimental data and colored curves are deconvolution fits. The fitting results are listed in Table S3.
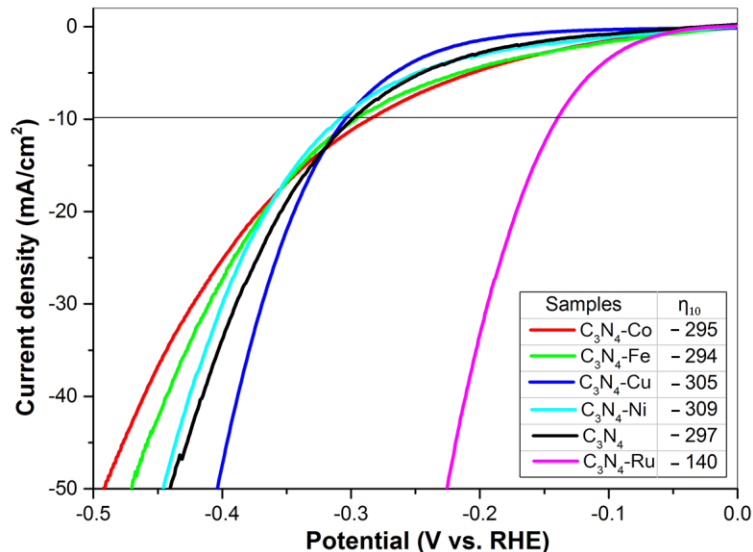
Figure S7. HER performance of the C_3N_4-M nanocomposites (M = Fe^{2+}, Co^{2+}, Ni^{2+} and Cu^{2+}). As indicated in the figure legends, the overpotentials (η_{10}) needed to reach the current density of 10 mA/cm^2 were all very close to that of C_3N_4 alone and much more negative than that of C_3N_4-Ru-F. This indicates the unique contributions of Ru ions to the HER activity, whereas minimal from other metal ions.
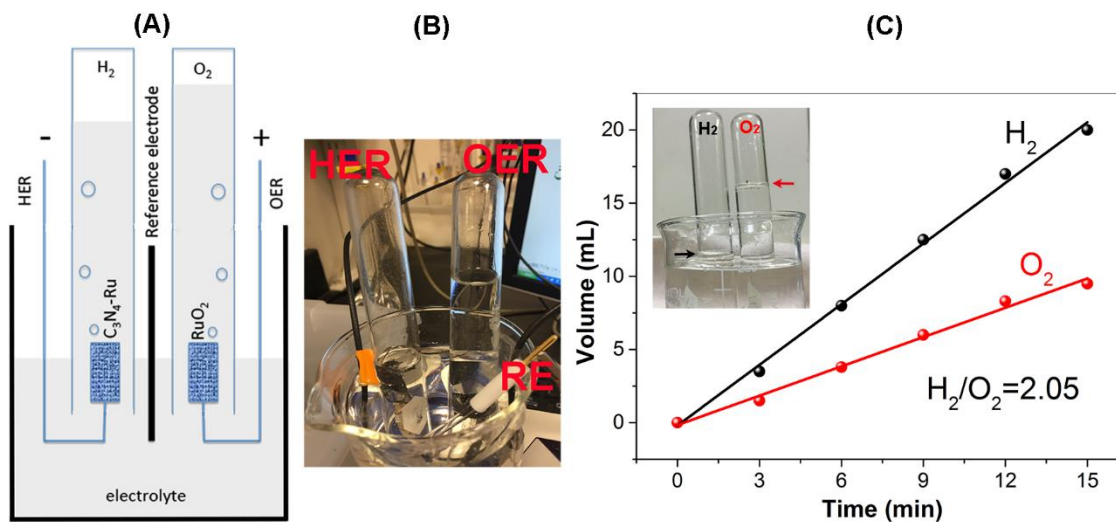

Figure S8. (A) Schematic illustration of the full water splitting cell setup. (B) Photograph of the home-made water splitting setup. (C) Results of water displacement during 20 min of electrochemical operation. Inset is the photograph of water displacement after 20 min.
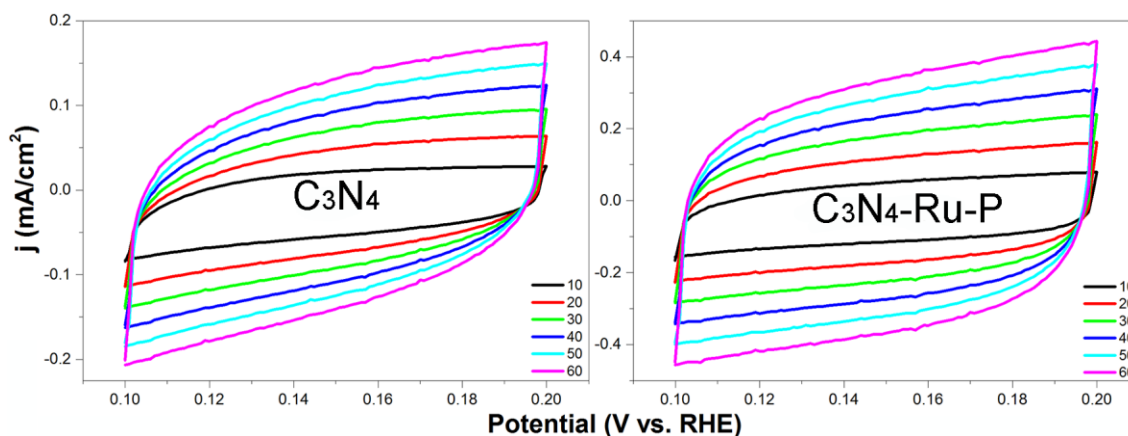
Figure S9. Cyclic voltammograms of C_3N_4 (right) and C_3N_4-Ru-P (left) within the range of +0.1 to +0.2 V at difference scan rates (10-60 mV/s), where no faradaic reaction occurred.
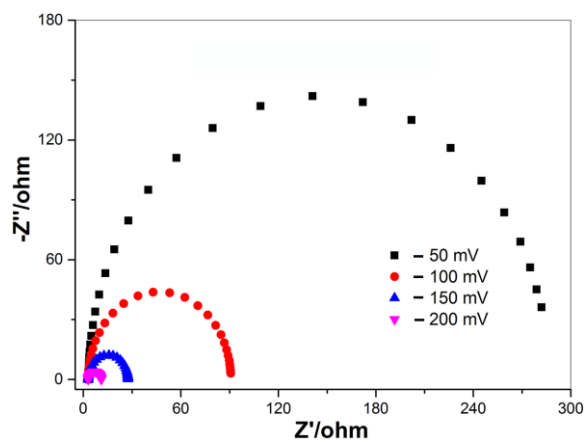

Figure S10. Nyquist plots of HER on C_3N_4-Ru-F at different overpotentials (-50, -100, -150 and -200 mV).
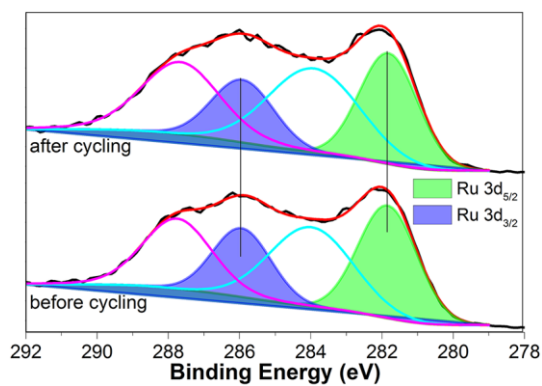

Figure S11. XPS spectra of the C 1s and Ru 3d electrons in C_3N_4-Ru-F before and after 1000 electro-chemical cycles.
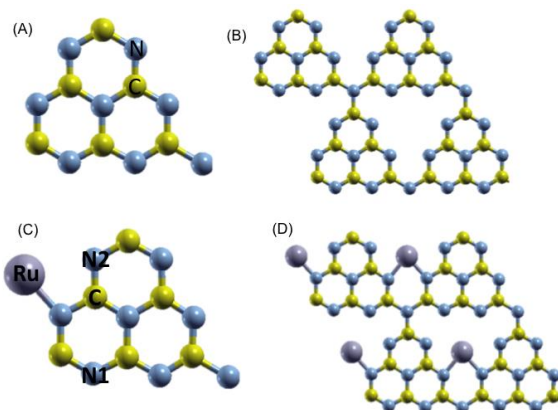
Figure S12. (A) 1×1 and (B) 2×2 cell structures of C_3N_4. (C) 1×1 and (D) 2×2 cell structures of C_3N_4-Ru. In these cell structures, the labeled atoms will be used as the targets to calculate the Gibbs free-energy for hydrogen adsorption (ΔG_{H^*}). The molecular configurations are obtained after relax calculations, and coordination of ruthenium ions is based on experimental data (Figure 2). For the calculations in (C) and (D), only the possible active sites are chosen and similar sites are ignored.
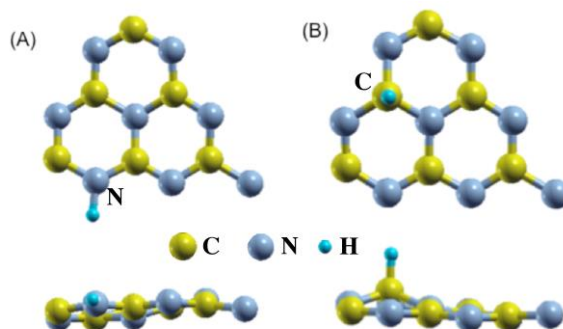

Figure S13. Stable hydrogen adsorption on labeled (A) N and (B) C of C_3N_4 after relax calculation. Tops are topic view and bottoms are side view.
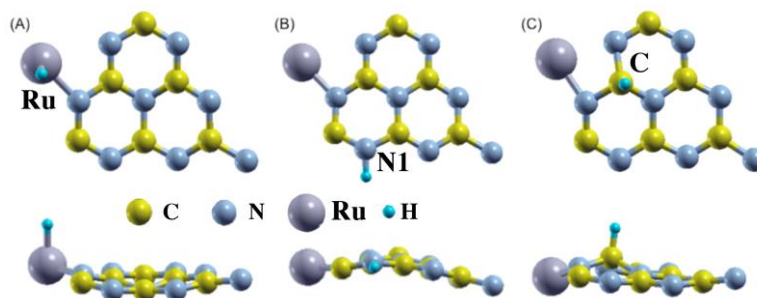

Figure S14. Stable hydrogen adsorption on labeled (A) Ru, (B) N1, and (C) C of C_3N_4-Ru after relaxing calculations. Tops are topic view and bottoms are side view. For N sites, the results of N1 and N2 are similar, so only one of them is shown here.